Focal Adhesion Protein FAP52 Self-Associates through a Sequence Conserved among the Members of the PCH Family Proteins†

Marko Nikki,‡ Jari Meriläinen,§ and Veli-Pekka Lehto*,‡,||

Department of Pathology, University of Oulu, FIN-90014 Oulu, Finland, Laboratory Technologies Division, Thermo Labsystems OY, FIN-00881 Helsinki, Finland, and Department of Pathology, University of Helsinki, FIN-0029 Helsinki, Finland

Received November 29, 2001; Revised Manuscript Received February 4, 2002

ABSTRACT: FAP52 is a recently described focal adhesion-associated protein. It is a member of an emerging PCH (*p*ombe *C*dc15 *h*omology) family of proteins characterized by a common domain organization and involvement in actin cytoskeleton organization, cytokinesis, and vesicular trafficking. Using gel filtration, surface plasmon resonance, and native polyacrylamide gel electrophoresis analysis, combined with chemical cross-linking of both native and recombinant protein, we show that FAP52 self-associates in vitro and suggest that it occurs predominantly as a trimer also in vivo. Analysis of the various domains of FAP52 by surface plasmon resonance showed that the highly α-helical region in the N-terminal half of the protein provides the self-association interface. Overexpression of the oligomerization domain in cultured cells was accompanied by major alterations in cellular morphology, actin organization, and the structure of focal adhesions, suggesting that an orderly coming together of FAP52 molecules is crucial for a proper actin filament organization and cytoskeletal structure. Comparison of the primary structures shows that all of the members of the PCH family have, in their N-terminal halves, a similar, highly α-helical region, suggesting that they all have a capacity to self-associate.

FAP52 (*f*ocal *a*dhesion *p*rotein of *52*000 daltons) is a recently characterized focal adhesion-associated protein which, in immunofluorescence microscopy (IFM),[1] colocalizes with vinculin, talin, and paxillin (*1*). It has a distinct three-domain structure with a highly α-helical N-terminal half and a C-terminal SH3 domain interspersed by a nonglobular linker region. By these structural features and sequence similarity, it belongs to a larger family of proteins which currently include the following members: EM13 of *Echinococcus multilocularis*, EG13 of *Echinococcus granulosus* (*2*), Cdc15 (*3*) and Imp2 (*4*) of *Schizosaccharomyces pombe*, Hof1/Cyk2 (*5*, *6*) of *Saccharomyces cerevisiae*, and the mammalian or avian proteins PSTPIP 1, a proline−serine−threonine phosphatase-interacting protein (*7*), CD2BPI, a CD2 cytoplasmic tail-binding protein (*8*), CIP4, a Cdc42-interacting protein (*9*), PACSIN (isoforms 1, 2, and 3; *10*), and syndapin (isoforms I and II; *11*). With Cdc15 as the founding member, this family of proteins is known as the *p*ombe *C*dc15 *h*omology (PCH) family (*12*). MAYP, a macrophage actin-associated tyrosine-phosphorylated protein (*13*), and its homologue PSTPIP 2 (*14*) are similar to PSTPIP except for the lack of the SH3 domain. PCH family members are also characterized by the presence of an N-terminal FER-CIP4 homology (FCH) domain (*9*) and a proline−glutamic acid−serine−threonine (PEST) sequence close to the SH3 domain in most members. Some of the proteins, for instance, FAP52, also have one or several NPF motifs, known for their role as EH-binding motifs in some other proteins (*15*). On the basis of the sequence similarities, FAP52, PACSIN 2, and syndapin II are homologous proteins. FAP52 is most similar to a short isoform of syndapin II (syndapin II-s) and PACSIN 2 to a long isoform of syndapin II (syndapin II-l). Due to a high degree of sequence similarity, this group of proteins is also called the syndapin protein family (*16*) with FAP52 as its founding member.

The specific locational and functional features of FAP52/PACSIN/syndapin are still only partially known. They are all widely expressed in various tissues. FAP52 associates with focal adhesions (*1*). PACSIN 2, on the other hand, is found in vesicular structures and in partial codistribution with actin filaments and microtubule network when overexpressed (*17*). Syndapin II, in turn, colocalizes with the endocytic machinery in neuroendocrine cells and is involved in multiple protein−protein interactions at the synaptic vesicles (*16*). Thus, despite a high degree of sequence similarity, syndapin family members show distinctly different subcellular distributions and divergent functional associations. Their modular

† This work was supported by the Finnish Academy and the Finnish Cancer Research Fund.

* To whom correspondence should be addressed. E-mail: lehto@csc.fi. Fax: 358-8-5375953. Phone: 358-8-5375950.

‡Department of Pathology, University of Oulu.

§ Thermo Labsystems OY.

|| Department of Pathology, University of Helsinki.

[1] Abbreviations: IFM, immunofluorescence microscopy; SH3, Src homology 3; PCH, pombe Cdc15 homology; FCH, Fer-CIP4 homology; PEST, proline−glutamic acid−serine−threonine; GST, glutathione *S*-transferase; PCR, polymerase chain reaction; aa, amino acid(s); HA, hemagglutinin; CEHF, chicken embryo heart fibroblast; PBS, phosphate-buffered saline; DSS, disuccinimidyl suberate; DMSO, dimethyl sulfoxide; NPAGE, nondenaturing polyacrylamide gel electrophoresis; IB, immunoblotting; ECL, enhanced chemiluminescence; FPLC, fast protein liquid chromatography; BSA, bovine serum albumin; SPR, surface plasmon resonance; CD, circular dichroism; GST, glutathione; CBB, Coomassie Brilliant Blue; NC, nitrocellulose.

10.1021/bi015991n CCC: $22.00
Published on Web 04/23/2002

architecture is suggestive of an adaptor function, and differences in the interactions mediated by the distinct domains may underlie their different locational and functional features.

Focal adhesions are highly complex multimolecular assemblies with a multitude of structural proteins involved in multiple protein−protein interactions (*18*). Via its SH3 domain, FAP52 could conceivably be part of such complexes. Other binding sites in FAP52 for interacting proteins could be its two NPF motifs and the N-terminal end which has a predicted highly α-helical conformation. Theoretically, FAP52, via its N-terminus, could also self-associate and oligomerize, which could be important, e.g., for sequestration of proteins interacting with the SH3 domain, NPF motifs, or other regions of FAP52.

Here we have investigated the supramolecular organization of FAP52 and show that it self-associates and probably forms trimers both in vitro and in vivo. By using transfection experiments, we demonstrate that interference with the oligomerization of FAP52 leads to changes in cell morphology and in actin and focal adhesion organization. We also show that the N-terminal coiled-coil region is crucial for the homophilic oligomerization. On the basis of sequence comparisons, we further propose that all of the members of the PCH family share a capacity to self-associate and oligomerize.

EXPERIMENTAL PROCEDURES

General Procedures and Computer Programs. The solutions, buffers, and procedures for standard purification and precipitation of DNA and for restriction enzyme digestions and ligations of cDNAs were as described in Sambrook et al. (*19*). Production and purification of the recombinant proteins in BL21(DE3) cells were performed according to standard procedures recommended by Amersham Pharmacia Biotech. DNA sequencing was carried out by using automated sequencing. For sequence alignments, the program Clustal X, version 1.8 (*20*), was utilized. For the prediction of the location of coiled-coil regions, the programs PairCoil (*21*) and MultiCoil (*22*) were employed at the network servers http://nightgale.lcs.mit.edu/cgi-bin/score and http://nightingale.lcs.mit.edu/cgi-bin/multicoil, respectively.

Affi-K7. Rabbit polyclonal antibody to bacterially produced FAP52, denoted Affi-K7, was produced and affinity-purified as described elsewhere (*1*).

cDNA Constructs. Full-length and truncated forms of FAP52 were produced as fusion proteins with glutathione *S*-transferase (GST) in BL21(DE3) cells by employing the vectors pGEX-2TK and pGEX-2T (Amersham Pharmacia Biotech). For that purpose, a 1.35 kb cDNA, encoding the full-length FAP52, was inserted into the *Bam*HI/*Eco*RI cloning site in the vector. The cDNAs encoding for the specific domains of FAP52 were prepared by PCR utilizing oligonucleotide primers with engineered restriction sites matching those of the cloning sites in the vector. The resulting PCR products were digested with *Bam*HI and *Eco*RI and ligated into the corresponding sites of the pGEX-2T or pGEX-2TK vector.

The cDNAs used for the transfection experiments in cultured cells were produced by PCR. In the PCR reaction, a 3′ primer with an extension specifying a 9 amino acid (aa) long hemagglutinin (HA) epitope tag was employed. cDNAs encoding the full-length FAP52 and its N-terminus were produced and cloned into the *Eco*RI/*Eco*RV cloning site of a pRK5 vector (a gift from Dr. J. Schlessinger; New York University Medical Center, New York). The authenticities of all the cDNA constructs were verified by sequencing.

Transfections and Cell Lysates. Chicken embryo heart fibroblasts (CEHF) were prepared, grown, and lysed as described previously (*1*). Transfections were carried out by using a Fugene 6-transfection reagent (Boehringer Mannheim) and following the manufacturer's instructions.

Chemical Cross-Linking. For chemical cross-linking, 25 μL of the bacterially produced protein (0.15 mg/mL) in PBS, or the clarified CEHF lysate (0.15 mg/mL), was incubated in the presence or absence of 1 μL of 10 mM disuccinimidyl suberate (DSS) in DMSO for 10 min at room temperature. The reaction was terminated by addition of 6 μL of the SDS−PAGE loading buffer into the reaction mixture.

Gel Filtration Chromatography. Bacterially produced FAP52 (1 mg/mL) in PBS or clarified CEHF lysate (0.75 mg/mL) was applied on a Superdex 200 gel filtration column connected to the FPLC system. The sample was eluted with PBS with a flow rate of 0.5 mL/min, and the run was monitored by absorbance at 280 nm. The peak fractions (sample volume 1 mL) were collected and analyzed by SDS−PAGE and IB.

Immunoblotting. Immunoblotting (IB) and enhanced chemiluminescence (ECL) were carried out essentially as described earlier (*1*). As primary antibodies, Affi-K7 or anti-GST and, as secondary antibodies, peroxidase-conjugated anti-rabbit IgG or anti-mouse IgG, respectively, were used.

Surface Plasmon Resonance. Surface plasmon resonance (SPR) measurements were performed on a BIACORE 3000 analyzer (Biacore AB) controlled by a BIACORE control software, version 3.1.1. Anti-GST antibody was immobilized on a carboxymethyl-coated CM5 sensor chip by employing the GST capture kit and the amine coupling kit (Biacore AB). For coating with the GST−FAP52 fusion protein, the chip was incubated with the fusion protein (0.15 mg/mL in 10 mM sodium acetate, pH 5.5) for 30 s with a flow rate of 30 μL/min. The chip was then equilibrated with HBS−EP buffer [0.01 M HEPES, pH 7.4, 0.15 M NaCl, 3 mM EDTA, 0.005% (v/v) polysorbate 20]. Bacterially produced FAP52 at concentrations of 20, 50, 100, 200, and 400 nM or fragments thereof at a concentration of 0.01 mg/mL in HBS−EP were passed over the chip with a flow rate of 30 μL/min. The injection volume was 30 μL. To correct the sensorgrams for background binding and bulk refractive index changes, a different flow cell without the immobilized GST−FAP52 was used as a reference. As controls, GST-coated chips were used onto which FAP52 was passed at a concentration of 100 nM. Kinetics was analyzed by BIAevaluation software, version 3.1.

Far-UV Circular Dichroism (CD). For CD experiments, the protein was dialyzed against 50 mM potassium phosphate buffer, pH 7.4. The concentration was then adjusted to approximately 0.2 mg/mL. The CD value scans were measured from 190 to 260 nm, at a step resolution of 2 nm and with a scanning rate of 20 nm/min. The CD spectra were the average of 10 scans. The content of α-helicity was calculated by employing a Protein Secondary Structure Program, Model SSE338 (Jasco Research; *23*).

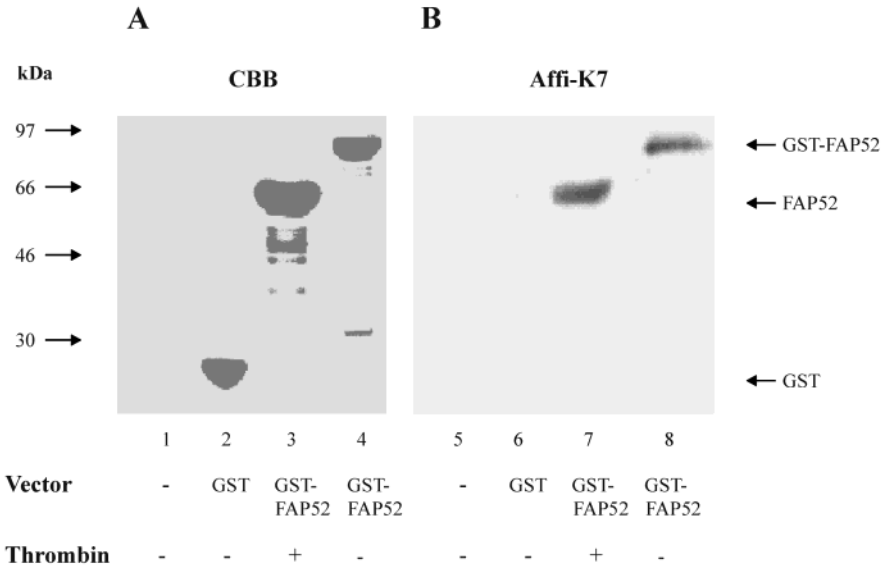

FIGURE 1: Purification and characterization of bacterially produced FAP52 and GST−FAP52. SDS−PAGE followed by (A) CBB staining or (B) IB of proteins purified from bacteria containing no vector (lanes 1 and 5), GEX-2TK vector with no insert (lanes 2 and 6), or GEX-2TK vector containing a cDNA encoding FAP52 (lanes 4 and 8). Protein extracts from the induced bacteria were affinity-purified on GT−Sepharose. In lanes 3 and 7, the affinity-purified material was subjected to thrombin digestion prior to the run. Equal amounts of protein were separated on SDS−PAGE in parallel runs. Lanes 1−4 were processed for CBB staining. Lanes 5−8 were transferred to a nitrocellulose (NC) membrane and probed using Affi-K7. Molecular mass markers are shown on the left-hand side.

Immunofluorescence Microscopy. CEHF cells were grown on glass coverslips, fixed, and stained as described elsewhere (*1*). In cases with staining of actin filaments, postfixation was carried out with ethanol for 1 min. As primary antibodies, rabbit polyclonal anti-HA or mouse monoclonal anti-paxillin and, as secondary antibodies, fluorophore-conjugated anti-rabbit or anti-mouse IgG, respectively, were used at appropriate dilutions. Fibrous actin was visualized with rhodamine−phalloidin. Viewing was under a Zeiss LSM510 laser scanning microscope equipped with a Zeiss Axiovert 110M inverted microscope (Carl Zeiss Microscopy). The images were processed by using an LSM 3D software, version 5.2. (Carl Zeiss Microscopy).

RESULTS

Characterization of the GST−FAP52 Fusion Proteins. Figure 1 shows the protein staining (Figure 1A, lanes 1−4) and the corresponding (parallel run) IB with Affi-K7 (Figure 1B, lanes 5−8) of proteins purified, by using glutathione (GT)−Sepharose, from the induced and lysed bacteria carrying no vector (lanes 1 and 5) or vector constructs coding for GST (lanes 2 and 6) or for GST−FAP52 (lanes 3, 4, 7, and 8). After affinity purification, the material in lane 3 was subjected to thrombin digestion. In Coomassie Brilliant Blue (CBB) staining, no protein could be seen in the material affinity-purified from the control bacteria (lane 1). A single band of 27 kDa, corresponding to GST alone, a 63 kDa band corresponding to FAP52 released by thrombin from its fusion partner GST, and a 90 kDa band corresponding to GST−FAP52, were seen in panel A in lanes 2−4, respectively. IB with Affi-K7 (panel B) confirmed that the 63 kDa band in lane 3 and the 90 kDa band in lane 4 contain FAP52 and GST−FAP52, respectively.

In Figure 2, a schematic representation of the domain organization of FAP52 is shown, accompanied by schematic representations of the constructs used in this work (Figure 2A).

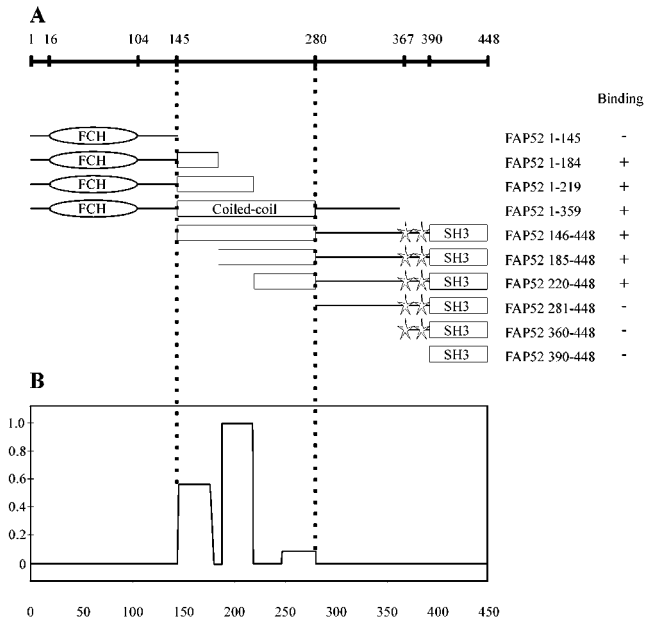

FIGURE 2: Domain structure of FAP52 and the deletion constructs. (A) Schematic representation of the predicted domains and motifs of FAP52: FCH domain, aa 16−104, coiled-coil region, aa 146−280, two NPF motifs, aa 367−369, 378−380, and SH3 domain, aa 390−448. Diagrams of the various deletion mutants are shown. The mutants are named as FAP52 followed by the first and the last residue expressed. On the right-hand site, SPR screening to determine the self-association domain in FAP52 is shown by plus (+) or minus (−), indicating the presence or absence of binding. (B) PairCoil plot of FAP52 reveals three distinct regions with a high probability to form coiled coils.

Recombinant FAP52 Self-Associates in Solution. The potential for oligomerization and the oligomeric status of the recombinant FAP52 in solution were determined by three different methods: SDS−PAGE of cross-linked FAP52, nondenaturing polyacrylamide gel electrophoresis (NPAGE), and gel filtration.

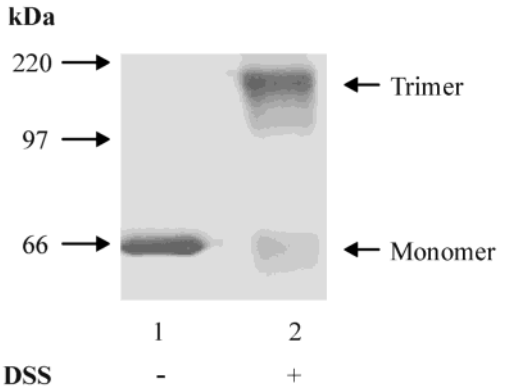

FIGURE 3: Cross-linking and SDS−PAGE. FAP52 was released from the GT−Sepharose-bound GST−FAP52 fusion protein by thrombin digestion. The purified protein was then mock-treated (lane 1) or cross-linked with DSS (lane 2) and analyzed by SDS−PAGE and CBB staining. Molecular mass markers are indicated on the left-hand side.

As a first step to analyze the oligomeric state of FAP52, chemical cross-linking of the recombinant FAP52 was done followed by SDS−PAGE and CBB staining. Figure 3 shows that the cross-linked FAP52 migrated as two distinct bands of molecular masses 170 and 63 kDa (lane 2). They correspond to a trimultiple and a unit molecular mass of FAP52, respectively, suggesting that in solution FAP52 occurs predominantly as a trimer. Non-cross-linked FAP52, on the other hand, was seen as a single band of 63 kDa (lane 1). Under similar conditions, cross-linking of unrelated proteins did not yield covalent oligomers (not shown).

To determine the nature of the native state of FAP52 in solution, we also employed NPAGE and size exclusion gel chromatography followed by IB with Affi-K7. In contrast to SDS−PAGE in which detergent forces the molecules to dissociate from their interactions, these techniques preserve the protein−protein interactions and, thus, give insight into the subunit structure of multimeric proteins. In both assays, a trimeric form of 170 kDa was detected. Moreover, a prominent and a weaker 350 kDa species was seen in NPAGE and gel chromatography, respectively, most probably representing hexameric forms of FAP52 (data not shown). Overall, the above experiments demonstrate the capacity of FAP52 to self-associate and suggest the formation of mostly trimeric and also higher oligomeric forms in solution.

Kinetics of FAP52 Self-Association. The interaction and the kinetics of the FAP52 self-association were studied by means of a real time SPR analysis with BIACORE. To do that, we first determined the conditions under which the immobilized GST−FAP52 only occurs as a monomer. This was done by incubating the recombinant FAP52 in buffers with various salt concentrations and pHs, followed by chemical cross-linking and SDS−PAGE analysis. It was established that in salt-free sodium acetate, pH 5.5, FAP52 remains monomeric and that oligomerization starts occurring at pH 6.5 and with increasing salt concentrations (data not shown). On the basis of this screening, coating of the chip was done in 10 mM sodium acetate, pH 5.5.

To carry out a real time analysis of self-association, a series of concentrations of FAP52 (from 20 to 400 nM) were injected over the derivatized chip. Distinct changes in a response in sensorgrams were observed when FAP52 was passed over immobilized GST−FAP52 (Figure 4). The difference between the RU values at the beginning and the cessation of the analyte injection, marking the initiation of association and dissociation, respectively, is an indication of a binding of FAP52 in the solution to the anchored GST−FAP52. The association rate was estimated to be 1.15×10^5 M^{-1} and the dissociation rate 5.47×10^{-4} M, giving an apparent affinity of 4.7×10^{-9} M. In the control, with GST instead of GST−FAP52 immobilized onto the chip, followed by FAP52 injection, no response was detected.

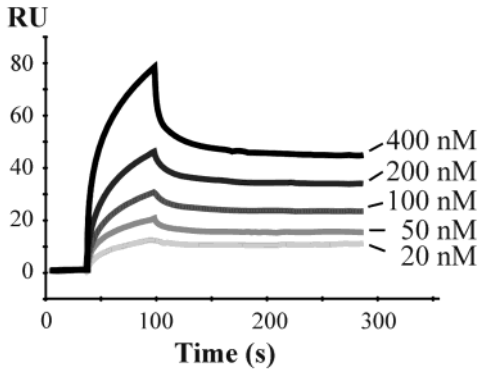

FIGURE 4: Surface plasmon resonance analysis. Sensorgrams showing the binding of FAP52 to GST−FAP52 which was coupled to immobilized anti-GST antibody. FAP52 in PBS was passed over the anchored GST−FAP52 at concentrations of 20, 50, 100, 200, and 400 nM. Each kinetic cycle involved a 1 min association phase, a 5 min dissociation phase, and a 2 min regeneration phase (with 20 mM glycine, pH 2.2; not shown). Experiments were carried out at 20 °C with a flow rate of 30 μL/min.

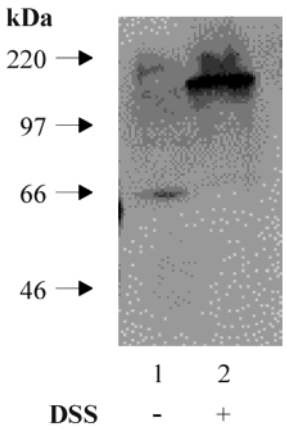

FIGURE 5: Cross-linking and IB of FAP52 in vivo. A clarified whole cell lysate from CEHF was either mock-treated (lane 1) or cross-linked with DSS (lane 2) and subjected to SDS−PAGE followed by IB using Affi-K7.

FAP52 Forms Oligomers in Vivo. To study the oligomeric state of the endogenous FAP52 in cells, we utilized IB with Affi-K7 of both the cross-linked whole cell lysate and the fractions from the size exclusion chromatography of a non-cross-linked lysate.

Figure 5 shows the IB analysis of the whole cell lysate of cultured CEHFs that was cross-linked with DSS (lane 2), with non-cross-linked species as a control (lane 1). After cross-linking, FAP52 migrates with a molecular mass of 170 kDa while in the non-cross-linked sample it displays a unit mass of 63 kDa. This indicates that, in intact cells, FAP52 occurs predominantly in an oligomeric, most probably a trimeric, form.

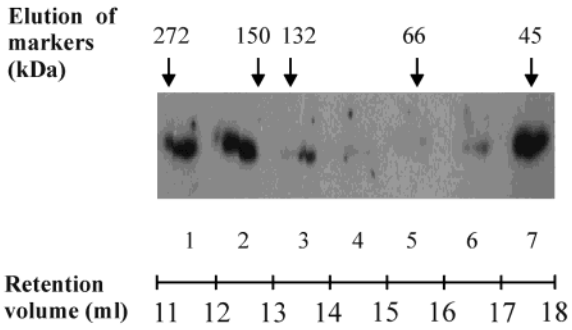

FIGURE 6: Gel filtration and IB of the CEHF lysate. The CEHF lysate was passed through a Superdex 200 gel filtration column, and 1 mL fractions were collected (lane 1, 11−12 mL; lane 2, 12−13 mL; lane 3, 13−14 mL; lane 4, 14−15 mL; lane 5, 15−16 mL; lane 6, 16−17 mL; lane 7, 17−18 mL) on the basis of the elution profile of the gel filtration of the recombinant FAP52 under identical conditions. The retention volume is shown by the ruler at the bottom and the elution of the molecular mass markers by arrows on the top. Aliquots of the fractions were subjected to SDS−PAGE. After a transfer of the polypeptides to the NC filter, FAP52 in the fractions was detected by IB with Affi-K7. From the position in the elution profile the molecular mass of the native FAP52 in the cell lysate was determined.

Figure 6 shows the IB of the fractions of the cell lysate collected from the Superdex 200 column. The majority of FAP52 eluted at a retention volume of 11−13 mL (lanes 1 and 2) and a minority at a volume of 17−18 mL (lane 7). This corresponds to the molecular masses of 170 and 60 kDa, respectively, as determined from the elution profile of the markers, supporting the suggestion that FAP52 in cells occurs in a multimeric form.

Mapping of the Self-Association Site of FAP52. Next we wanted to delineate the region in FAP52 that is responsible for the self-association. For that purpose, we employed SPR with GST−FAP52 immobilized on the chip and various 5′ and 3′ deletion mutants of FAP52 in the mobile phase. Figure 7 shows the responses observed when the various truncated forms of FAP52 were passed over the immobilized GST−FAP52. A distinct binding was seen with all of the N-terminal fragments of FAP52 except for the one encompassing residues 1−145. Among the C-terminal fragments, on the other hand, binding was seen up to a truncation at a level of amino acid residue 281. This effectively attributes the self-association function of FAP52 to the region spanning amino acids 146−280. Distinct binding was also seen with fragments 1−184 and 220−448. This suggests that several distinct regions within a span of 146−280 contribute to self-association.

Secondary Structure Prediction. Secondary structure prediction of FAP52 proposes a high propensity for α-helicity in the N-terminal two-thirds of FAP52 (*1*). Moreover, the heptad periodicity in this region and the conservation of several amino acid residues within the heptads suggest a coiled-coil organization and a propensity to form higher order oligomers (*1*, *24*). On the basis of this, we wanted to determine whether a coiled-coil arrangement could underlie the propensity of the N-terminal region encompassing residues 146−280 to self-associate.

Figure 2B shows the probability of a coiled-coil arrangement of FAP52 as analyzed by the program PairCoil. The program predicts three regions comprising amino acid residues 146−179, 185−219, and 248−280, with probabilities of 53%, 100%, and 9%, respectively, to form coiled coils. This region matches exactly with the region which possesses the self-association capacity as determined by the SPR experiments. Another program, MultiCoil, predicts the propensities of these three regions to form trimers to be 4%, 10%, and 0.5% and dimers 3%, 74%, and 0%, respectively (not shown). From this, it can be concluded that a region spanning residues 146−280 and showing a high propensity to coiled-coil oligomerization accounts for the self-association capacity of FAP52.

Circular Dichroism. To verify the α-helical arrangement in the recombinant FAP52, we analyzed the recombinant full-length FAP52, its N-terminus (aa 1−359), and the C-terminal SH3 domain (aa 390−448) by CD (Figure 8). The CD spectra of the recombinant FAP52 and the N-terminus presented double minima at 208 and 220 nm and a maximum close to 212 nm. For the full-length FAP52, the molar ellipticity ratio $\theta_{220}/\theta_{208}$ was 1.04 ($-12.2 \times 10^{-4}/-11.7 \times 10^{-4}$), which is characteristic of an α-helical coiled coil (*25*). The extent of α-helicity was calculated to be 25.8%. The

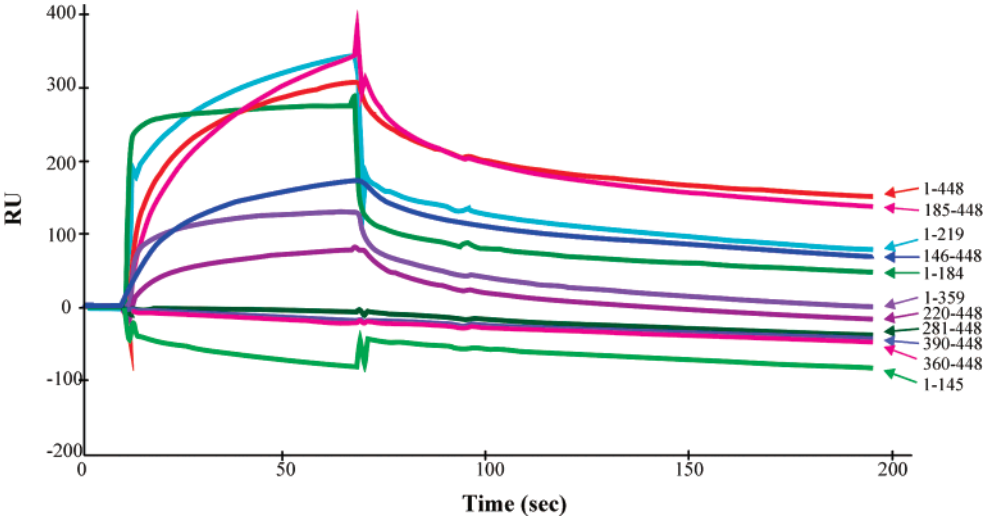

FIGURE 7: Mapping of the self-association site by SPR. Sensorgrams showing the binding of the truncated forms of FAP52 to immobilized GST−FAP52 were obtained by injecting 30 μL of the mutant protein at a concentration of 0.01 mg/mL and with a flow rate of 30 μL/min at 20 °C. Each kinetic cycle involved a 1 min association phase, a 5 min dissociation phase, and a 2 min regeneration phase.

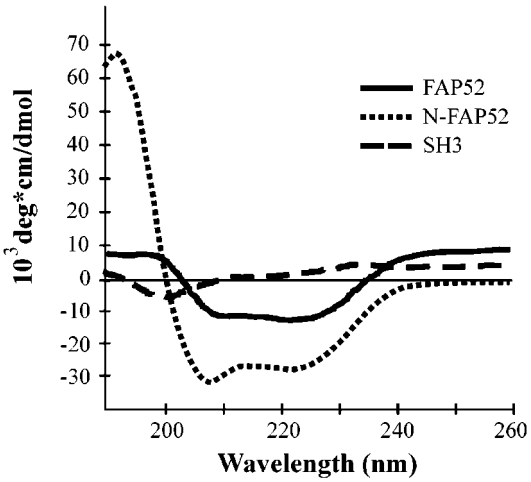

FIGURE 8: CD spectra of the affinity-purified (thrombin-released) FAP52 and the polypeptides corresponding to its N-terminal end (aa 1−359) and SH3 domain (aa 390−448).

SH3 domain of FAP52 exhibited only a single spectral minimum at 198 nm, suggesting a random coil conformation. The N-terminal fragment exhibited 57.7% α-helicity. Thus, the N-terminal half of FAP52 in solution shows the predicted high α-helical content. The results also indicate that the expressed recombinant fragments of FAP52 in solution adopt a conformation predicted by computer programs.

Transfection Experiments. To gain insight into the role of the self-association of FAP52 in cellular physiology, we transfected cells with the HA-tagged full-length FAP52 (FAP52−HA) (Figure 9a,b,d) and the N-terminal region which contains the self-association domain (aa 1−293; $FAP52_{Nt}$−HA) (Figure 9c). FAP52−HA was seen mostly widely distributed in the cytoplasm of the transfected cells without any predilection to associate with subcellular organelles (Figure 9a,b, green fluorescent cell in the right panel). However, an accentuated staining was seen in cell extensions and along the edges of the cell (Figure 9a,b, right panel, arrowheads). There were distinct changes in overall cell morphology in these transfected cells. Instead of an almost straight-edged contour seen in untransfected cells (indicated by asterisks in Figure 9a,b, left panel), many transfected cells displayed a highly undulating perimeter with many surface protrusions and often a bent morphology (Figure 9a,b, fluorescent cells in the right panels). Other categories of changes included cells with a more roundish morphology and an appearance compatible with a deficient spreading and cells with an almost needle-like, slender appearance and a tube-like cross section (not shown). Some transfectants were roundish and probably in the process of detaching from the substratum (not shown).

There were distinct differences also in the actin organization of the transfected vs normal cells, as revealed by double staining for actin with rhodamine−phalloidin of cell cultures transfected with FAP52−HA (Figure 9a,b, left panel). In nontransfected cells (indicated by asterisks), typical longitudinally oriented actin fibers were seen. In transfected cells (corresponding to the fluorescent cells in the right panels in a and b), a distinctly attenuated staining for actin was seen especially in the cells with a bipolar slender appearance and with several pseudopod-like protrusions (Figure 9a, left panel). On the other hand, there was a distinct filamentous

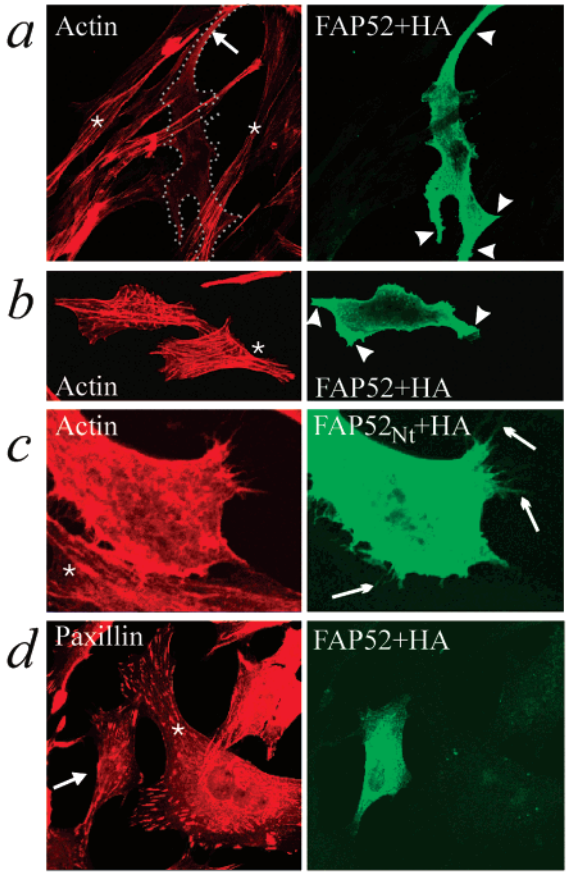

FIGURE 9: Immunofluorescence microscopy of CEHF cells overexpressing FAP52−HA or $FAP52_{Nt}$−HA. The cells were transfected with pRK5 expression vector encoding for HA epitope-tagged full-length FAP52 (a, b, and d) or HA epitope-tagged $FAP52_{Nt}$ (c). Double staining was with rhodamine−phalloidin for actin (left panel in a−c) or with anti-paxillin for paxillin (left panel in d) and with anti-HA for FAP52−HA (right panel in a, b, and d) or $FAP52_{Nt}$−HA (right panel in c). Asterisks denote nontransfected cells.

staining in the narrow funnel-like parts of the cell, probably representing the less motile trailing edge of the cell (Figure 9a, arrow). In the transfected cells with a phenotype resembling deficient spreading, there was usually some filamentous network to be seen (not shown). In some transfected cells, a filamentous actin network was seen which was, however, clearly in disarray with much more interconnections between the filaments and numerous brightly staining spot-like formations in the cytoplasm (cell corresponding to the fluorescent cell in the left panel of Figure 9b).

Also $FAP52_{Nt}$−HA showed a fairly uniform cytoplasmic distribution in transfected CEHFs (Figure 9c, fluorescent cell in the right panel). As a distinct feature of $FAP52_{Nt}$−HA transfected cells, extended cell protrusions with long, filopodia-like extensions were often seen (Figure 9c, arrows). In these cells, an attenuated or disarrayed actin network was seen when compared with nontransfected cells (asterisk) (Figure 9c, double staining for actin and $FAP52_{Nt}$−HA).

Since FAP52 is closely associated with focal adhesions, we also wanted to know whether and how focal adhesions in the transfected cells are affected. Therefore, double staining experiments were carried out employing anti-HA antibodies to detect overexpressed FAP52−HA (Figure 9d, right panel) or $FAP52_{Nt}$−HA (not shown) and anti-paxillin

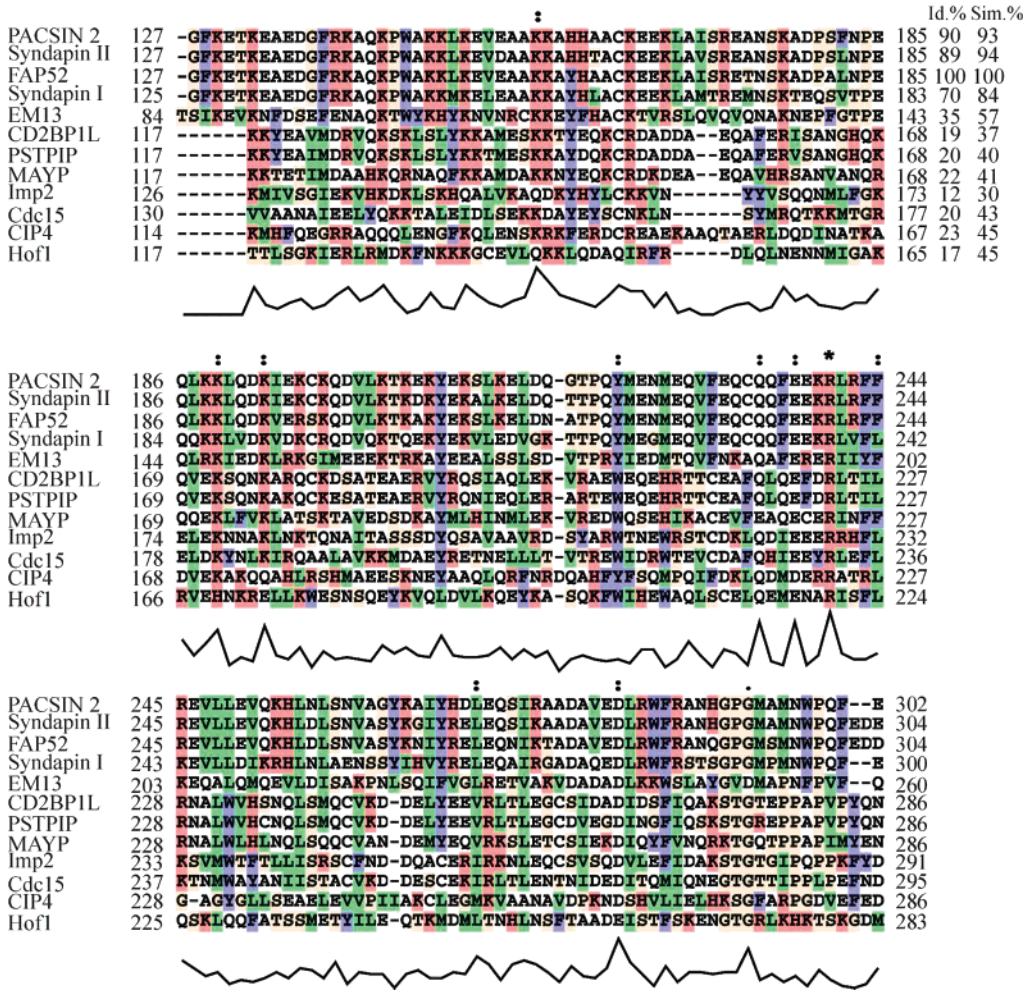

FIGURE 10: Multiple alignment of the members of PCH family using the Clustal X (1.8) program. The first column on the left shows the name of the protein. On the left, the number of the first amino acid residue is given. On the right, the number of the last residue on the line and the degree of sequence identity (Id.%) and similarity (Sim.%) with FAP52 are given. The single-letter code for amino acids is used. The residues are colored according to the following scheme: all glycines, serine, threonine, and prolines (G, S, T, P) are colored as brown. Other coloring is by the recurring feature: hydrophobic residues (V, M, I, L) are green; alanine, cysteine, and acidic and polar residues (A, D, E, N, C, Q) are left white; basic recidues (R, K, H) are red; and aromatic residues (F, Y, W) are blue. A single fully conserved residue is indicated by *, a strong conservation by ••, and weaker conservation by •. The conservation score for each column is indicated by the plot below the sequences. The SwissProt accession codes of the sequences are as follows: PACSIN2, q9UNF0; Syndapin II, q9qy20; FAP52, O13154; Syndapin I, q93UW5; EM13, q07840; CD2BP1L, O43586; PSTPIP, P97814; MAYP, QpZ189.sp_rodent; Imp2, YBY2 SCHPO; Cdc15, q09822.swissprot; CIP4, O15184; Hof1, cyk2_yeast.

antibodies (Figure 9d, left panel) to decorate focal adhesions. Similar changes were seen in cells overexpressing FAP52 or $FAP52_{Nt}$. In general, distinct focal adhesions were seen in both types of overexpressers as judged by immunodetection with anti-paxillin antibodies. Compared to the nontransfected cells, however, they often showed aberrant morphology in being usually small and with distorted morphology (Figure 9d, left panel; asterisk, nontransfected cell; arrow, transfected cell). Often their arrangement was abnormal; instead of being regularly spaced and oriented radially in the peripheral parts of the cells, they were often seen in disarray.

Comparison of the N-Terminal Domains of the Members of PCH Family of Proteins. FAP52, along with its close relatives PACSIN 2 and syndapin II, belongs to a family of PCH proteins which share a common domain organization. There is a high degree of sequence similarity (30−94%) and identity (12−90%) in the N-terminal region, ranging from 131 to 299, in all of these proteins, as shown in the alignment analysis by the Clustal X program (Figure 10). In PairCoil analysis, a high propensity to coiled-coil arrangement was predicted for all of the aligned sequences (not shown). These results suggest that also other members of the PCH family may have a capacity to oligomerize through their α-helical N-terminal region.

DISCUSSION

Several biochemical and biophysical techniques convincingly showed that FAP52 in solution has a capacity to self-associate. The results also suggest that it predominantly forms homotrimers. By using sequentially truncated mutant forms of the recombinant protein, the self-association site could be localized to a highly α-helical region encompassing amino acid residues 146−280. This suggests coiled-coil arrangement as the basis of oligomerization.

From SPR measurements, a self-association binding affinity of 4.7×10^{-9} M could be calculated on the premise that only monomer-to-monomer binding takes place between the analyte and the ligand. Taking into account that self-

association takes place also in the solution (*26*), the binding constant of 4.7×10^{-9} M can be considered to represent a minimum value of the binding affinity. Thus, as a rough estimation, it can be concluded that FAP52 self-associates at an affinity higher than $k_D = 4.7 \times 10^{-9}$ M.

The calculated k_D of 4.7×10^{-9} M is indicative of a stable oligomerization of FAP52. In SPR analysis, it is manifested as a rapid interaction even at low concentrations and as a slow dissociation. A similar small k_D is also seen with many coiled-coil dimers with different primary sequences and with proteins forming either heterodimers [Fos/Jun; $(20-100) \times 10^{-9}$ M; *27*] or homodimers (bZIP protein VBP; 14×10^{-9} M; *28*). Similar high affinities have been found also in heterophilic coiled-coil formation in a study in which also the use of SPR for such studies was validated (*29*).

The distinct predominance of one oligomerization state of FAP52 is fully in line with what is seen with other coiled-coil proteins. Thus, for instance GICN4 leucine zipper is commonly used as a model of dimer formation while heat shock transcription factors serve as a model system to study trimeric coiled-coil formation (*24*, *30*). The determinants for the putatively triple-stranded coiled-coil arrangement of FAP52 are most probably embedded in specific features of the typical heptad repeat structure of the oligomerization region such as, for instance, the occurrence of polar side chain amino acids serine and threonine characteristically in the *d* or *g* positions of the repeats (*31*, *32*). Further work is, however, needed to establish whether the determinants reside exclusively within this region or whether the oligomerization state is also affected by flanking sequences, for instance, in the case of the heat shock transcription factor (*33*). More detailed studies are also underway to resolve the degree and mechanism of oligomerization; whether it involves cooperative transition from the monomer, as suggested by the current data, or whether there are different oligomeric states that could represent intermediate or equilibrium states.

Major morphological changes were seen in cells overexpressing either a full-length FAP52 or a polypeptide containing the self-association domain of FAP52. It included attainment of an aberrant overall morphology. Most prominently, the cells displayed numerous cell surface protrusions which were either lamellipodium-like broad-based extensions or slender and long cell surface extensions which probably represent filopodia. The overall impression of the morphological changes was that, in transfected cells, there were more and more prominent areas and structures which are indicative of high mobility. These include, e.g., pseudopod-like protrusions and filopodia (*34*, *35*). This correlates with the presence of a clearly attenuated stress fiber organization, typical of migratory cells (*34*). Since both pseudopods and filopodia, both present in transfected cells, are also actin-based structures (*36*, *37*), it seems that what overexpression of FAP52 or $FAP52_{Nt}$ brings about is a change in the balance of factor(s) regulating the extent of polymerization of actin in various parts of a cell.

Filopodia are thin, spike-like formations which have actin filaments in their core (*38*). In fact, polymerization of actin is a prerequisite for their formation, and it can be induced, e.g., by overexpressing in cells Cdc42 or RalA, GTPases which regulate actin polymerization, or N-WASP (*39*−*41*). Thus, in regard to the close proximity of focal adhesions to the actin filaments and multiple physical links between focal adhesions and actin filaments, it is tempting to speculate that the overexpressed oligomerization domain of FAP52, by increasing the number of monomeric FAP52 (by way of displacing FAP52 from its oligomeric complex and/or by preventing FAP52 from self-associating), creates aberrant sites of actin polymerization at the cell surface. The loss of the regular filamentous actin organization, on the other hand, suggests that the aberrant expression of the oligomerization domain also disturbs the regular interaction, direct or indirect, between FAP52 and the actin fibers associated with the focal adhesion sites. The presence of focal adhesion sites at least in most overexpressors of FAP52 is intriguing. It could be explained on the basis that their integrity is not dependent on intact stress fibers (*42*, *43*). It also suggests that overexpression of FAP52 probably interferes with the focal adhesion−stress fiber linkage rather than the organization of focal adhesions per se.

Focal adhesions consist of a complex of proteins that assemble at sites of attachment of a cell to the extracellular matrix. Their formation is initiated by the engagement of the transmembrane protein integrins which, through their cytoplasmic tails, provide linkages to the actin cytoskeleton. While clearly a hierarchical process, the binding kinetics between integrins and their cytoskeleton-associated binding partners are poorly known (*44*). Only recently, a systematic screening on kinetic aspects of several integrin ($\alpha IIb\beta 3$) binding proteins was done (*45*). It showed that the binding affinity of talin, filamin, F-actin, and α-actinin ranged from 0.4 to 5 μM. Although studied in platelets, these results compare well with the data obtained by other means (*46*−*50*). Overall, these data suggest that cytoskeletal proteins in focal adhesions interact with a modest or weak affinity. This may be a requirement for versatility and velocity of the assembly and disassembly of the linkages, dictated by the demands of the cell motility and transient adhesion (*51*). The high-affinity self-association of FAP52, on the other hand, suggests that FAP52 is constitutively present as an oligomer in an intact cell, as, in fact, was strongly indicated by the cross-linking experiment in which FAP52 in cell lysate was seen almost exclusively in oligomeric form. Thus, it seems, but remains to be established by further studies, that the major regulatory step in the incorporation of FAP52 into the syntax of focal adhesions is not its oligomerization but, rather, its recruitment, as an oligomer, into contact with its interacting partners.

Despite a common architectural design, the members of the PCH family seem to be involved in quite different cellular functions. Syndapins take part in vesicle trafficking in neural and other types of cells (*16*). PACSIN acts in endocytosis (*17*, *52*). PSTPIP is involved in cytokinesis (*7*). The roles of Cdc15 (*3*) and Imp2 (*4*) in *S. pombe* are also associated with cytokinesis. Cyk2 of the budding yeast is instrumental in the budding process (*6*). Despite these to all appearances disparate functions, all of these proteins are in some ways associated with events involving the regulation of the actin cytoskeleton; according to Lippincott and Li (*12*), they may have a general involvement in actin-based functions. Thus, for instance, localization of PSTPIP and PSTPIP2 (MAYP) in actin-rich areas suggests a general involvement in actin-based events (*7*, *14*). CIP4, on the other hand, binds activated

Cdc42, a GTPase that is an important regulator of actin polymerization (*9*). Also the functions of the PCH proteins that are involved in cytokinesis are either spatially or functionally closely associated with actin filaments which contribute in a critical way to the formation of the cleavage furrow and the progress of cytokinesis (*4*, *6*, *53*).

Syndapin II, a close homologue of FAP52, and the related syndapin I are implicated as components of the endocytic machinery. They are, however, also clearly involved in actin dynamics, as recently shown by Qualmann and Kelly (*16*). Overexpression of both syndapin I and syndapin II dramatically altered actin organization in cultured cells, inducing long filopodia similar to those seen in $FAP52_{Nt}$-transfected cells in this study. The full-length syndapin was needed for this effect; the SH3 domain or the N-terminal portion did not have the same effect. From the double transfection experiments it was learned that the effects on actin are most probably mediated by the Arp2/3 complex and N-WASP, notorious for their role in the regulation of actin polymerization. N-WASP binds to the SH3 domain of both syndapin I and syndapin II (*16*). Thus syndapins most probably link endocytosis and actin dynamics. In accordance with this, Modregger et al. (*52*) showed recently that also all of the three known isoforms of PACSIN are involved in the endocytic process and that also they bind N-WASP. They also showed, by using a yeast two-hybrid system and an ELISA-style ligand-binding assay, that all three isoforms were capable of homo- and heteroassociation. The assay was done by using full-length proteins, and the predicted highly α-helical N-terminal region was considered as the association interface.

A highly α-helical region with a propensity to coiled-coil arrangement, as predicted by a secondary structure analysis, is to be found in the N-terminal part of all PCH family members. In some proteins it adjoins the very N-terminal FCH domain which is present in many proteins unrelated to the PCH members and which is not involved in the self-association of FAP52. The coiled-coil domains in PCH proteins show a high degree of similarity, ranging from 30% to 94%. Such a high degree of conservation of an α-helical domain is surprising knowing that, when embedded within related multidomain proteins, the coiled-coil domains usually show the lowest degree of sequence similarity (*54*). It strongly suggests that not only FAP52 but also the other PCH members have a capacity to self-associate. The conservation further suggests that the α-helical domain in the PCH proteins displays structural constraints dictated by specific functional or interaction features that go beyond the mere maintenance of the characteristic polar/apolar sequences that is needed for α-helix formation. Such specific features could involve either homooligomerization or heteroassociation restricted exclusively to the members of the same family.

ACKNOWLEDGMENT

We thank Dr. Päivi Pirilä and Dr. Kalervo Hiltunen for advice and invaluable help with surface plasmon resonance analysis, Dr. Matti Vuento for CD analysis, and Ms. Marjaana Vuoristo, Ms. Marja Tolppanen, Ms. Marja-Liisa Martti, Ms. Tarja Piispanen, and Mr. Hannu Wäänänen for skillful technical assistance.

REFERENCES

1. Meriläinen, J., Lehto, V.-P., and Wasenius, V.-M. (1997) *J. Biol. Chem. 272*, 23278−23284.
2. Frosch, P. M., Geier, C., Kaup, F. J., Muller, A., and Frosch, M. (1993) *Mol. Biochem. Parasitol. 58*, 301−310.
3. Fankhauser, C., Reymond, A., Cerutti, L., Utzig, S., Hofmann, K., and Simanis, V. (1995) *Cell 82*, 435−444.
4. Demeter, J., and Sazer, S. (1998) *J. Cell Biol. 143*, 415−427.
5. Kamei, T., Tanaka, K., Hihara, T., Umikawa, M., Imamura, H., Kikyo, M., Ozaki, K., and Takai, Y. (1998) *J. Biol. Chem. 273*, 28341−28345.
6. Lippincott, J., and Li, R. (1998) *J. Cell Biol. 143*, 1947−1960.
7. Spencer, S., Dowbenko, D., Cheng, J., Li, W., Brush, J., Utzig, S., Simanis, V., and Lasky, L. A. (1997) *J. Cell Biol. 138*, 845−860.
8. Li, J., Nishizawa, K., An, W., Hussey, R. E., Lialios, F. E., Salgia, R., Sunder-Plassmann, R., and Reinherz, E. L. (1998) *EMBO J. 17*, 7320−7336.
9. Aspenström, P. (1997) *Curr. Biol. 7*, 479−487.
10. Plomann, M., Lange, R., Vopper, G., Cremer, H., Heinlein, U. A., Scheff, S., Baldwin, S. A., Leitges, M., Cramer, N., Paulsson, M., and Barthels, D. (1998) *Eur. J. Biochem. 256*, 201−211.
11. Qualmann, B., Roos, J., DiGregorio, P. J., and Kelly, R. B. (1999) *Mol. Biol. Cell 10*, 501−513.
12. Lippincott, J., and Li, R. (2000) *Microsc. Res. Technol. 49*, 168−172.
13. Yeung, Y. G., Soldera, S., and Stanley, E. R. (1998) *J. Biol. Chem. 273*, 30638−30642.
14. Wu, Y., Dowbenko, D., and Lasky, L. A. (1998) *J. Biol. Chem. 273*, 30487−30496.
15. Salcini, A. E., Confalonieri, S., Doria, M., Santolini, E., Tassi, E., Minenkova, O., Cesareni, G., Pelicci, P. G., and Di Fiore, P. P. (1997) *Genes Dev. 11*, 2239−2249.
16. Qualmann, B., and Kelly, R. B. (2000) *J. Cell Biol. 148*, 1047−1062.
17. Ritter, B., Modregger, J., Paulsson, M., and Plomann, M. (1999) *FEFS Lett. 454*, 356−362.
18. Sastry, S. K., and Burridge, K. (2000) *Exp. Cell Res. 261*, 25−36.
19. Sambrook, J., Fritsch, E. F., and Maniatis, T. (1989) *Molecular Cloning: A Laboratory Manual*, 2nd ed., Cold Spring Harbor Laboratory, Cold Spring Harbor, NY.
20. Thompson, J. D., Gibson, T. J., Plewniak, F., Jeanmougin, F., and Higgins, D. G. (1997) *Nucleic Acids Res. 25*, 4876−4882.
21. Berger, B., Wilson, D. B., Wolf, E., Tonchev, T., Milla, M., and Kim, P. S. (1995) *Proc. Natl. Acad. Sci. U.S.A. 92*, 8259−8263.
22. Wolf, E., Kim, P. S., and Berger, B. (1997) *Protein Sci. 6*, 1179−1189.
23. Yang, J. T., Wu, C.-S., and Martinez, H. M. (1986) *Methods Enzymol. 130*, 208−269.
24. Kohn, W. D., Mant, C. T., and Hodges, R. S. (1997) *J. Biol. Chem. 272*, 2583−2586.
25. Zhou, N. E., Kay, C. M., and Hodges, R. S. (1992) *J. Biol. Chem. 267*, 2664−2670.
26. Mavaddat, N., Mason, D. W., Atkinson, P. D., Evans, E. J., Gilbert, R. J., Stuard, D. I., Fennelly, J. A., Barclay, A. N., Davis, S. J., and Brown M. H. (2000) *J. Biol. Chem. 275*, 28100−28109.
27. Patel, L. R., Curran, T., and Kerppola, T. K. (1994) *Proc. Natl. Acad. Sci. U.S.A. 91*, 7360−7364.
28. Krylov, D., Mikhailenko, I., and Vinson, C. (1994) *EMBO J. 13*, 2849−2861.
29. Chao, H., Houston, M. E., Grothe, S., Kay, C. M., O'Connor-McCourt, M., Irvin, R. T., and Hodges, R. S. (1996) *Biochemistry 35*, 12175−12185.
30. Thomas, R. M., Zampieri, A., Jumel, K., and Harding, S. E. (1997) *Eur. Biophys. J. 25*, 405−410.

31. Shu, W., Ji, H., and Lu, M. (1999) *Biochemistry 38*, 5378−5385.
32. Woolfson, D. N., and Alber, T. (1995) *Protein Sci. 4*, 1596−607.
33. Drees, B. L., Grotkopp, E. K., and Nelson, H. C. (1997) *J. Mol. Biol. 273*, 61−74.
34. Couchman, J. R., and Rees, D. A. (1979) *J. Cell Sci. 39*, 149−165.
35. Small, J. V., Rottner, K., Kaverina, I., and Anderson, K. I. (1998) *Biochim. Biophys. Acta 1404*, 271−281.
36. Mallavarapu, A., and Mitchison, T. (1999) *J. Cell Biol. 146*, 1097−1106.
37. Svitkina, T. M., and Borisy, G. G. (1999) *J. Cell Biol. 145*, 1009−1026.
38. Condeelis, J. (1993) *Annu. Rev. Cell Biol. 9*, 411−444.
39. Ohta, Y., Suzuki, N., Nakamura, S., Hartwig, J. H., and Stossel, T. P. (1999) *Proc. Natl. Acad. Sci. U.S.A. 96*, 2122−2128.
40. Miki, H., Sasaki, T., Takai, Y., and Takenawa, T. (1998) *Nature 391*, 93−96.
41. Castellano, F., Montcourrier, P., Guillemot, J. C., Gouin, E., Machesky, L., Cossart, P., and Chavrier, P. (1999) *Curr. Biol. 9*, 351−360.
42. Pavalko, F. M., and Burridge, K. (1991) *J. Cell Biol. 114*, 481−491.
43. Cattelino, A., Albertinazzi, C., Bossi, M., Critchley, D. R., and de Curtis, I. (1999) *Mol. Biol. Cell 10*, 373−391.
44. Miyamoto, S., Teramoto, H., Coso, O. A., Gutkind, J. S., Burbelo, P. D., Akiyama, S. K., and Yamada, K. M. (1995) *J. Cell Biol. 131*, 791−805.
45. Goldmann, W. H. (2000) *Biochem. Biophys. Res. Commun. 271*, 553−557.
46. Otey, C. A., Pavalko, F. M., and Burridge, K. (1990) *J. Cell Biol. 111*, 721−729.
47. Pavalko, F. M., and LaRoche, S. M. (1993) *J. Immunol. 151*, 3795−3807.
48. Knezevic, I., Leisner, T. M., and Lam, S. C. (1996) *J. Biol. Chem. 271*, 16416−16421.
49. Burridge, K., and Mangeat, P. (1984) *Nature 308*, 744−746.
50. Turner, C. E., Glenney, J. R., and Burridge, K. (1990) *J. Cell Biol. 111*, 1059−1068.
51. van der Merwe, P. A., and Barclay, A. N. (1994) *Trends Biochem. Sci. 19*, 354−358.
52. Modregger, J., Ritter, B., Witter, B., Paulsson, M., and Plomann, M. (2000) *J. Cell Sci. 113*, 4511−4521.
53. Imamura, H., Tanaka, K., Hihara, T., Umikawa, M., Kamei, T., Takahashi, K., Sasaki, T., and Takai, Y. (1997) *EMBO J. 16*, 2745−2755.
54. Lupas, A., Van Dyke, M., and Stock, J. (1991) *Science 252*, 1162−1164.

BI015991N